


Nonstationary dynamics of the sine lattice consisting of three pendula (trimer)

Margarita Kovaleva, Valery Smirnov, and Leonid Manevitch
Semenov Institute of Chemical Physics, Russian Academy of Sciences, Moscow, Russia

 (Received 25 December 2017; revised manuscript received 3 December 2018; published 11 January 2019)

The low- and high-amplitude oscillations in the system of three nonlinear coupled pendula (trimer) are analyzed beyond the quasilinear approximation. The considered oscillations are fundamental for many models of the energy exchange processes in physical, mechanical, and biological systems, in particular, for the torsional vibrations of flexible polymers or DNA's double strands. We obtained the conditions of the basic stationary solutions' stability. These solutions correspond to the nonlinear normal modes (NNMs), the instability of which leads to the appearance of localized NNMs (stationary energy localization). Using an asymptotic procedure, we reduce the dimension of the system's phase space that allows us to analyze the energy exchange between pendula in the slow timescale and to reveal periodic interparticle energy exchange and nonstationary energy localization. It has been shown recently that essentially nonstationary resonance processes of this type are adequately described in terms of the limiting phase trajectories (LPTs) corresponding to beatings between the oscillators or coherence domains in the slow timescale. Moreover, it turns out that criteria of the transition to the stationary and nonstationary energy localization can be formulated as the bifurcation conditions for NNMs and LPTs, respectively. The trimer under consideration is a nonintegrable system, and therefore its equations of motion is only after dimensions reduction can be analyzed by the Poincare sections method. Finally, we aim to study the highly nonstationary regimes, which correspond to beatinglike periodic or quasiperiodic recurrent energy exchange between the pendula.

DOI: [10.1103/PhysRevE.99.012209](https://doi.org/10.1103/PhysRevE.99.012209)

I. INTRODUCTION

The dynamics of coupled nonlinear oscillators have attracted the growing interest of the scientific community because of its fundamental meaning and various applications. Besides the early classic works which can be found in monographs [1–5] and more recent works [6,7], we can distinguish various types of the investigations. Many of them are devoted to the search for the periodic motions and cycles in the complex systems which comprise weakly coupled subsystems [8–10], including proofs of the existence and stability of the 2π -periodic motions, but without the construction of the solutions themselves. There are also papers describing numerically the regimes existing in the systems of the identical oscillators with different coupling types [11,12]. Another special series of investigations on synchronization of the coupled oscillators is based on the phase approximation [13–15] and quasilinear approach [16,17]. These works are based on the assumption of the small amplitude modulations of the oscillators. Analysis of the stability of the NNMs and construction of the analytical solutions in the vicinity of the equilibrium state of two pendula with weak or strong linear coupling has been made in [18–20]. If the amplitude modulations are not small, the approach based on the nonlinear normal modes (NNMs) and limiting phase trajectories (LPTs) appears to be very effective [21–39]. The limiting phase trajectories are defined as phase trajectories showing the maximum possible energy exchange between the parts of the system [i.e., between the oscillators, the oscillatory clusters (coherence domains), or between the system and external field] [25,26]. Evolution of the LPTs

in the parametric space allows prediction of the thresholds corresponding to the dynamic transition. In the case of strongly modulated processes, the analytical description can be obtained in terms of nonsmooth basic functions. The efficient solution of the nonstationary problem for two linearly coupled pendula without restrictions on the amplitudes of oscillations is presented in [27].

The model of the coupled nonlinear pendula with the sine-type nonlinear coupling (we will denote it as a strongly nonlinear coupling) serves as an adequate model for many physical systems such as paraffin crystals, ferromagnetic chains, and many organic molecules, including DNA [28,29]. In the paper, we consider one of the simplest cases of this type, namely, the system of three identical pendula coupled via a strongly nonlinear potential. With the example of the Fermi-Pasta-Ulam chain [30,31], we have already shown that under the resonant conditions, the coherent domains (clusters), which interact weakly, play the role of the oscillators in the energy exchange and energy localization processes. The dynamics of the clusters in the framework of the two degrees of freedom model is reduced to the dynamics of the oscillators themselves.

Our work concerns the case with more than two degrees of freedom. As the chain has free boundary conditions, the symmetry between the middle element of the chain and the side elements is broken. Therefore, the short chain of three pendula with strongly nonlinear coupling is studied separately. Up to now, the case of three- and four-element chains was considered for the rotors only [32,33]. In these works, the analytical solutions are studied and a comparison of the

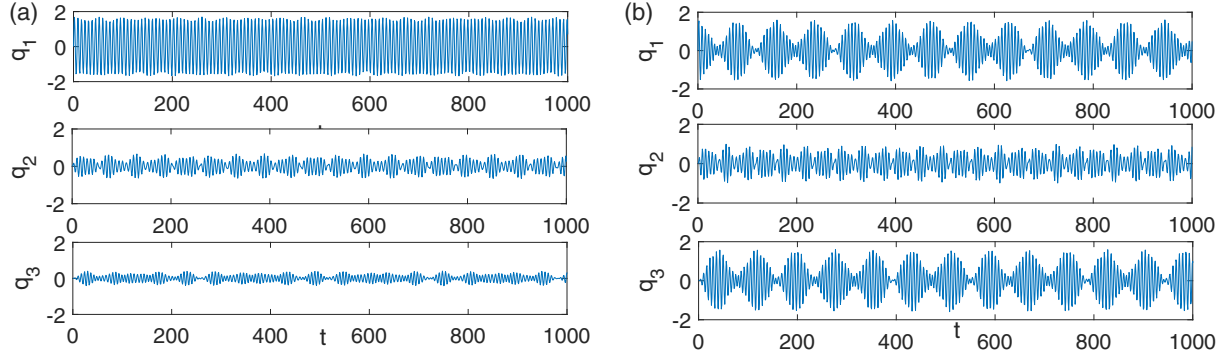


FIG. 1. Energy transport regimes for the initial excitation of the first element equal to $Q = \frac{\pi}{2}$; parameter values: (a) $\beta = 0.1$, (b) $\beta = 0.2$.

localized regimes with well-known discrete breathers is made [35]. These results could be compared with the study of our system in the limit of rotating pendula. However, in our study, we focus only on the large-amplitude oscillations but not rotations.

In the current paper, in contrast to many works devoted to interacting nonlinear oscillators, the nonlinearity of both the pendula and the coupling between them are not assumed to be small. Thus, the research methods that involve quasilinearity and the presence of a small parameter characterizing nonlinearity and/or coupling are not applicable. To overcome this difficulty, a semi-inverse method was proposed [36]. Using this method and the LPT concept, the system of two identical

linearly and strongly nonlinearly coupled pendula was examined under different oscillation amplitudes [26,37]. Stationary and nonstationary transitions leading to a qualitative change in the dynamic behavior of the system were analytically described. This work continues the previous investigations for the more complex case, when the coupling between the pendula cannot be assumed weak and the number of degrees of freedom is equal to three.

II. THE MODEL AND ASYMPTOTIC PROCEDURE

The Hamiltonian of the system of three identical pendula coupled via the cosine potential in the dimensionless form can be represented as follows:

$$H = \sum_{j=1,2,3} \left\{ \frac{1}{2} \left(\frac{dq_j}{dt} \right)^2 + [1 - \cos(q_j)] \right\} + \beta[1 - \cos(q_2 - q_3)] + \beta[1 - \cos(q_2 - q_1)], \quad (1)$$

$$\begin{aligned} \frac{d^2 q_1}{dt^2} + \beta \sin(q_1 - q_2) + \sin(q_1) &= 0, & \frac{d^2 q_2}{dt^2} + \beta \sin(q_2 - q_1) + \beta \sin(q_2 - q_3) + \sin(q_2) &= 0, \\ \frac{d^2 q_3}{dt^2} + \beta \sin(q_3 - q_2) + \sin(q_3) &= 0. \end{aligned} \quad (2)$$

The main difference of the system (2) from the system of two coupled pendula is that there is a significant symmetry break: the middle element is under action of the coupling with two neighboring oscillators, while the side elements are coupled only once. The periodic boundary conditions would make the situation more symmetric, but we concentrate our study on the planar model.

Let us first look at the possible energy transport regimes similarly to the system of two strongly nonlinearly coupled pendula [37]. For that, we set the initial conditions

$$q_1 = 0; \quad q_2 = 0; \quad q_3 = 0; \quad \dot{q}_1 = Q; \quad \dot{q}_2 = 0; \quad \dot{q}_3 = 0;$$

and change of the coupling parameter β in a wide range, where Q is the initial excitation (see Fig. 1). If the coupling is weak enough, the energy will stay on the initially excited side pendulum [see Fig. 1(a)]. However, if we increase the coupling over some threshold value, the regular energy transport between all three oscillators occurs [see Fig. 1(b)]. Let us note that only the system of three nonlinear oscillators with a “soft” type of nonlinearity can demonstrate such behavior. The trimer with hard nonlinearity can demonstrate regular recurrent energy transport only between two neighboring oscillators of the three elements of the chain [38]. To study the evolution of the energy transport states, we will use a semi-inverse method (see [27,36]) for application of the asymptotic procedure.

We suppose that the NNMs’ frequencies are close to each other, and the motion of the system happens with the frequency ω , which is also close to those of NNMs. The assumption of the closeness of the motion to the resonance with frequency ω allows

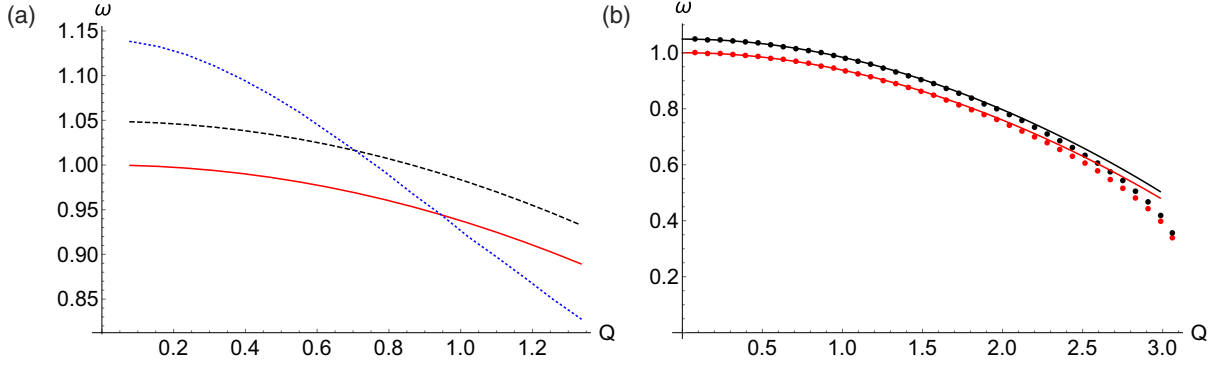


FIG. 2. The NNM frequencies vs the NNM's amplitudes. Coupling parameter $\beta = 0.1$. (a) Numerical demonstration of the frequency inversion, different NNMs are presented by colors: in-phase (1,1,1) red solid line; (1,0,-1) black dashed line; (1,-2,1) blue dotted line. (b) Comparison of the analytical solution with the numerical results for in-phase (red lower line) mode and antiphase (1,0,-1) (black upper line) mode. Solid lines define the analytical results; dots correspond to results obtained numerically from the initial system.

rewriting the system in the following form:

$$\begin{aligned} \frac{d^2 q_1}{dt^2} + \omega^2 q_1 + \varepsilon \mu [-\omega^2 q_1 + \sin(q_1)] + \varepsilon \beta_0 \sin(q_1 - q_2) &= 0, \\ \frac{d^2 q_2}{dt^2} + \omega^2 q_2 + \varepsilon \mu [-\omega^2 q_2 + \sin(q_2)] + \varepsilon \beta_0 \sin(q_2 - q_1) + \varepsilon \beta_0 \sin(q_2 - q_3) &= 0, \\ \frac{d^2 q_3}{dt^2} + \omega^2 q_3 + \varepsilon \mu [-\omega^2 q_3 + \sin(q_3)] + \varepsilon \beta_0 \sin(q_3 - q_2) &= 0, \end{aligned}$$

where ε is a small parameter and μ is a bookkeeping parameter, so that $\varepsilon \mu = 1$, and $\varepsilon \beta_0 = \beta$.

We introduce complex variables $\psi_j = \frac{1}{\sqrt{2}} \left(\frac{1}{\sqrt{\omega}} \frac{dq_j}{dt} + i \sqrt{\omega} q_j \right)$, where ω is a still undefined frequency of the resonant motion. We also represent the sine function as an infinite sum of the following complex argument:

$$\begin{aligned} i \frac{d}{dt} \psi_1 + \omega \psi_1 + \varepsilon \mu \left[-\frac{\omega}{2} (\psi_1 + \psi_1^*) + \frac{i}{\sqrt{2\omega}} \sum \frac{(-1)^k}{(2k+1)!} \left(\frac{-i}{\sqrt{2\omega}} \right)^{2k+1} (\psi_1 - \text{c.c.})^{2k+1} \right] \\ + \frac{i \varepsilon \beta_0}{\sqrt{2\omega}} \sum \frac{(-1)^k}{(2k+1)!} \left(\frac{-i}{\sqrt{2\omega}} \right)^{2k+1} (\psi_1 - \psi_2 - \text{c.c.})^{2k+1} &= 0, \\ i \frac{d}{dt} \psi_2 + \omega \psi_2 + \varepsilon \mu \left[-\frac{\omega}{2} (\psi_2 + \psi_2^*) + \frac{i}{\sqrt{2\omega}} \sum \frac{(-1)^k}{(2k+1)!} \left(\frac{-i}{\sqrt{2\omega}} \right)^{2k+1} (\psi_2 - \text{c.c.})^{2k+1} \right] \\ + \frac{i \varepsilon \beta_0}{\sqrt{2\omega}} \sum \frac{(-1)^k}{(2k+1)!} \left(\frac{-i}{\sqrt{2\omega}} \right)^{2k+1} [(2\psi_2 - \psi_1 - \psi_3) - \text{c.c.}]^{2k+1} &= 0, \\ i \frac{d}{dt} \psi_3 + \omega \psi_3 + \varepsilon \mu \left[-\frac{\omega}{2} (\psi_3 + \psi_3^*) + \frac{i}{\sqrt{2\omega}} \sum \frac{(-1)^k}{(2k+1)!} \left(\frac{-i}{\sqrt{2\omega}} \right)^{2k+1} (\psi_3 - \text{c.c.})^{2k+1} \right] \\ + \frac{i \varepsilon \beta_0}{\sqrt{2\omega}} \sum \frac{(-1)^k}{(2k+1)!} \left(\frac{-i}{\sqrt{2\omega}} \right)^{2k+1} (\psi_3 - \psi_2 - \text{c.c.})^{2k+1} &= 0. \end{aligned} \quad (3)$$

The value in brackets is supposed to be small, while the motion is close to the given frequency ω . Using a standard two-scale procedure, we separate “fast” $\tau_0 = t$ and “slow” $\tau_1 = \varepsilon \tau_0$ timescales: $\psi_j = \chi_{0,j}(\tau_0, \tau_1) + \varepsilon \chi_{1,j}(\tau_0, \tau_1)$, $j = 1, 2, 3$. Taking into account $\frac{d}{dt} = \frac{\partial}{\partial \tau_0} + \varepsilon \frac{\partial}{\partial \tau_1}$ and keeping only terms of the zeroth order of the small parameter, we obtain $\chi_{0,j} = \varphi_j(\tau_1) e^{i\omega t}$, $j = 1, 2, 3$. At the next step of the asymptotic procedure, we keep only terms of the first order of the small parameter, and supposing that we are looking only for limited solutions, we exclude resonating (secular) terms. The procedure yields the following set of

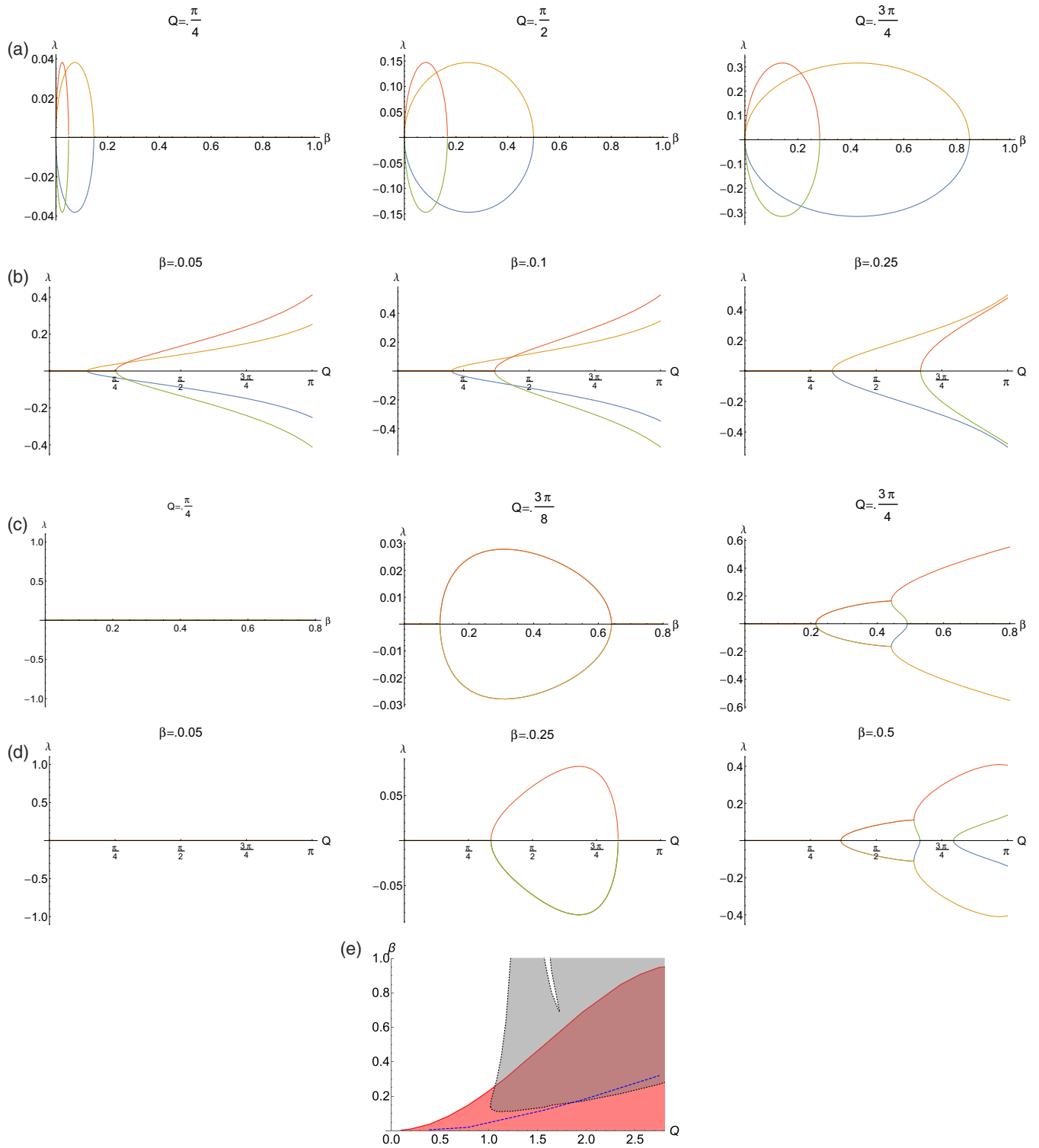


FIG. 3. Linear stability of the NNMs in the system (8): (a)–(d) Real parts of the eigenvalues of the Jacobian of linearized system (8) in the polar representation for the both interacting NNMs. (a) In-phase NNM for fixed values of initial excitation: $Q = \pi/4$, $Q = \pi/2$, $Q = 3\pi/4$. (b) In-phase NNM for fixed values of coupling: $\beta = 0.05$, $\beta = 0.1$, $\beta = 0.25$. (c) NNM (1,0,-1) for fixed values of initial excitation: $Q = \pi/4$, $Q = 3\pi/8$, $Q = 3\pi/4$. (d) NNM (1,0,-1) for fixed values of coupling: $\beta = 0.05$, $\beta = 0.25$, $\beta = 0.5$. (e) Instability regions for in-phase NNM (red solid line), NNM (1,0,-1) (gray, dotted line) compared with the localization-energy transport transition threshold (blue dashed line) obtained from system (1) with initial excitation Q placed only on the first element, same as in Fig. 1.

equations describing the evolution of the envelope functions in the slow timescale:

$$\begin{aligned}
i \frac{d}{d\tau_1} \varphi_1 + \mu \left[-\frac{\omega}{2} \varphi_1 + \frac{1}{\sqrt{2\omega}} J_1 \left(\sqrt{\frac{2}{\omega}} |\varphi_1| \right) \frac{\varphi_1}{|\varphi_1|} \right] + \frac{\beta_0}{\sqrt{2\omega}} J_1 \left(\sqrt{\frac{2}{\omega}} |\varphi_1 - \varphi_2| \right) \frac{\varphi_1 - \varphi_2}{|\varphi_1 - \varphi_2|} &= 0, \\
i \frac{d}{d\tau_1} \varphi_2 + \mu \left[-\frac{\omega}{2} \varphi_2 + \frac{1}{\sqrt{2\omega}} J_1 \left(\sqrt{\frac{2}{\omega}} |\varphi_2| \right) \frac{\varphi_2}{|\varphi_2|} \right] + \frac{\beta_0}{\sqrt{2\omega}} J_1 \left(\sqrt{\frac{2}{\omega}} |\varphi_2 - \varphi_1| \right) \frac{\varphi_2 - \varphi_1}{|\varphi_2 - \varphi_1|} \\
+ \frac{\beta_0}{\sqrt{2\omega}} J_1 \left(\sqrt{\frac{2}{\omega}} |\varphi_2 - \varphi_3| \right) \frac{\varphi_2 - \varphi_3}{|\varphi_2 - \varphi_3|} &= 0, \\
i \frac{d}{d\tau_1} \varphi_3 + \mu \left[-\frac{\omega}{2} \varphi_3 + \frac{1}{\sqrt{2\omega}} J_1 \left(\sqrt{\frac{2}{\omega}} |\varphi_3| \right) \frac{\varphi_3}{|\varphi_3|} \right] + \frac{\beta_0}{\sqrt{2\omega}} J_1 \left(\sqrt{\frac{2}{\omega}} |\varphi_3 - \varphi_2| \right) \frac{\varphi_3 - \varphi_2}{|\varphi_3 - \varphi_2|} &= 0,
\end{aligned} \tag{4}$$

where J_1 is Bessel function of the first kind.

The linear trimer of this type possesses three normal modes: one is an in-phase (1;1;1) mode, and two are different antiphase modes (1;0;-1) and (1;-2;1). For weak excitation levels, we can demonstrate numerically the frequency dependence on the amplitude of the initial excitation [see Fig. 2(a)]. It is evidently seen that there is an inversion of the spectrum with growth of the amplitude, namely, the frequency of the NNM (1,-2,1) has the highest frequency for weak excitation levels, but becomes the lowest frequency if the amplitudes are higher than 1 rad. This phenomenon cannot be observed in the system with linear coupling [27], but also is reported in the system of two pendula with cosine potential of interaction [37].

If the amplitude of the initial excitation is higher than $\pi/2$, only two of the NNMs survive. Therefore, only two of them can be found in the system (4), and we have found their frequencies:

$$\omega_i = \sqrt{\frac{2}{Q} J_1(Q)} \tag{5}$$

corresponds to in-phase mode;

$$\omega_a = \sqrt{\frac{2}{Q} (\beta + 1) J_1(Q)} \tag{6}$$

corresponds to mode (1;0;-1).

The comparison between asymptotic values (5) and (6) and the exact numerical results obtained from the initial system are presented in Fig. 2. It can be noted that for the low values of the coupling parameter β , the frequency of the NNM (1;0;-1) is close to the frequency of the in-phase NNM for a wide range of the excitation amplitudes. We see a very good

agreement between the exact and asymptotic results for the initial excitation values up to $Q = 9/10 \pi$. As we expected, the frequency of the oscillations decreases with the increase of the initial excitation (due to the soft nonlinearity effect). We should also emphasize that our assumption on the closeness of the NNM's frequencies appears to be valid for a wide range of the parameters and initial conditions. The obtained result defines the applicability of the semi-inverse method for our problem, which allowed introduction of the slow timescale.

Using the linearization procedure of (8) in the polar representation, the stability of both interacting NNMs can be examined (see Fig. 3). The polar representation allows one to consider only the amplitude instability of each of the NNMs, which is crucial for dynamical behavior. The analytical representation of the Jacobian is somewhat cumbersome, and therefore we omit it, presenting all the dependencies on the parameters of the system. We see that NNMs lose stability with growth of the coupling parameter β and/or the amplitude of excitation Q . However, this change of the phase space of the system cannot explain the transition from nonstationary energy localization to energy exchange presented in Fig. 1 [see Fig. 3(e)], as the transition occurs far below the stability loss of the in-phase mode and occurs even in the weak excitation region where the mode (1,0,-1) remains stable.

III. NONSTATIONARY DYNAMICS: POINCARÉ MAPS STUDY

To proceed with the study of the phase space, we intend to reduce the dimensionality of the model. Similarly to the system of two pendula [27,37], asymptotic system (4) possesses an additional integral of motion $X = \sum_{k=1}^3 |\varphi_k|^2$. It allows us to introduce spherical coordinates,

$$\varphi_1 = \sqrt{X} \cos \theta \cos \varphi e^{i\delta_1}, \quad \varphi_2 = \sqrt{X} \sin \theta e^{i\delta_2}, \quad \varphi_3 = \sqrt{X} \cos \theta \sin \varphi e^{i\delta_3}, \tag{7}$$

and using the fact that only the relative phases have physical meaning, we reduce the system to the form

$$\frac{d\theta}{d\tau_1} = \frac{\beta_0}{Q\omega} \frac{J_1(Q\sqrt{S_1})}{\sqrt{S_1}} \cos \varphi \sin \Delta_{12} - \frac{\beta_0}{Q\omega} \frac{J_1(Q\sqrt{S_2})}{\sqrt{S_2}} \sin \varphi \sin \Delta_{23},$$

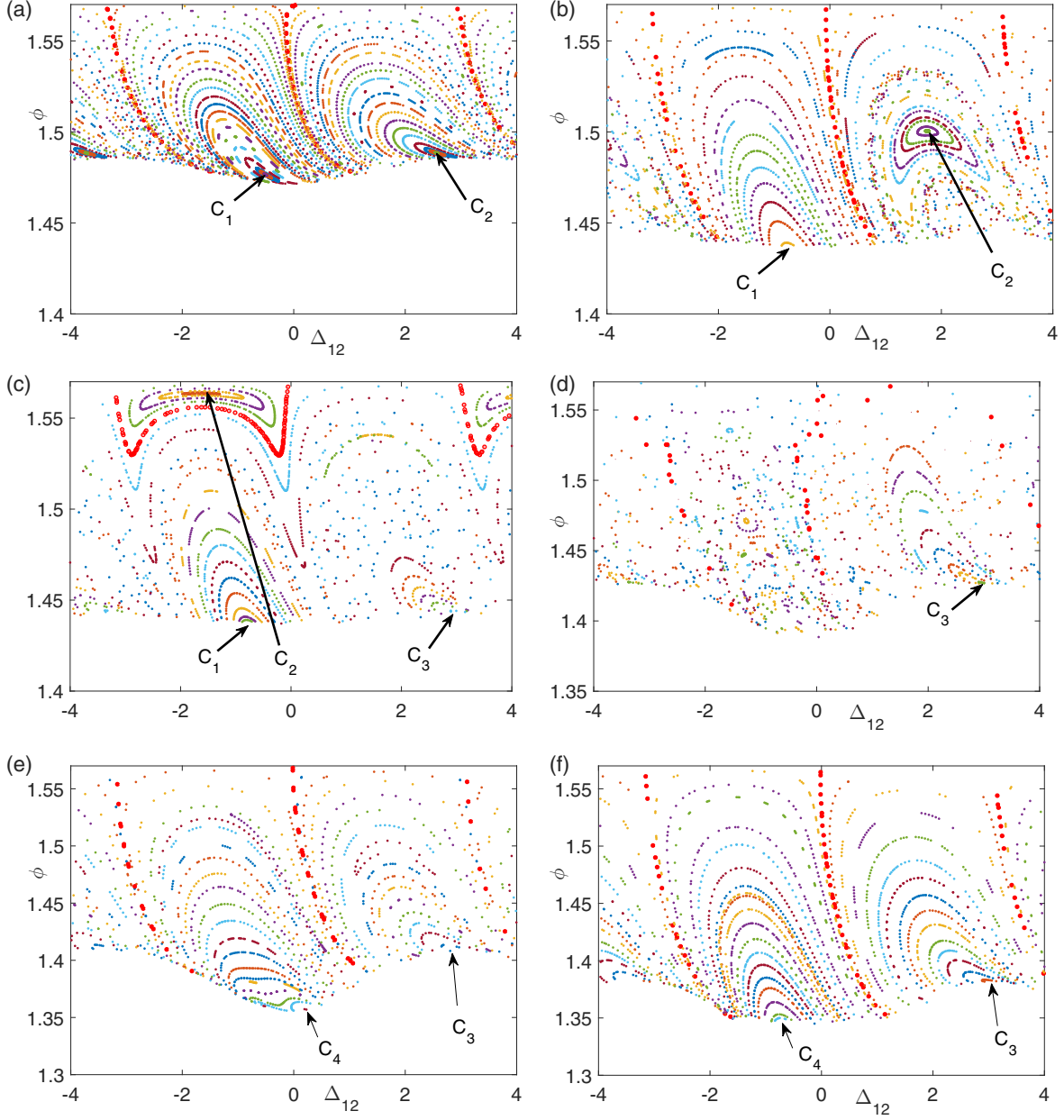


FIG. 4. Poincaré sections for the slow-flow system (8): $\theta = 1.53$, $\varepsilon = 0.1$, $\mu = 10$; (a) $\beta_0 = 0.5$; (b) $\beta_0 = 1.1$; (c) $\beta_0 = 1.13$; (d) $\beta_0 = 1.5$; (e) $\beta_0 = 2$; (f) $\beta_0 = 3$. Red bold points denote the phase orbit ELPT with initial conditions (10).

$$\begin{aligned}
 \frac{d\varphi}{d\tau_1} &= \frac{\beta_0}{Q\omega} \frac{J_1(Q\sqrt{S_1})}{\sqrt{S_1}} \tan \theta \sin \Delta_{12} \sin \varphi + \frac{\beta_0}{Q\omega} \frac{J_1(Q\sqrt{S_2})}{\sqrt{S_2}} \tan \theta \sin \Delta_{23} \cos \varphi, \\
 \sin 2\theta \frac{d\Delta_{12}}{d\tau_1} &= \frac{2\mu}{Q\omega} \left[J_1(Q \sin \theta) \cos \theta - \frac{J_1(Q \cos \theta \cos \varphi) \sin \theta}{\cos \varphi} \right] + \frac{2\beta_0}{Q\omega} \frac{J_1(Q\sqrt{S_1})}{\sqrt{S_1}} \left(\frac{\sin^2 \theta}{\cos \varphi} - \cos^2 \theta \cos \varphi \right) \cos \Delta_{12} \\
 &\quad + \frac{2\beta_0}{Q\omega} \frac{J_1(Q\sqrt{S_2})}{\sqrt{S_2}} \left(\frac{1}{2} \sin 2\theta - \cos^2 \theta \sin \varphi \cos \Delta_{23} \right), \\
 \sin 2\theta \frac{d\Delta_{23}}{d\tau_1} &= \frac{2\mu}{Q\omega} \left[-J_1(Q \sin \theta) \cos \theta + \frac{J_1(Q \cos \theta \sin \varphi) \sin \theta}{\sin \varphi} \right] - \frac{2\beta_0}{Q\omega} \frac{J_1(Q\sqrt{S_2})}{\sqrt{S_2}} \left(\frac{\sin^2 \theta}{\sin \varphi} - \cos^2 \theta \sin \varphi \right) \cos \Delta_{23} \\
 &\quad + \frac{2\beta_0}{Q\omega} \frac{J_1(Q\sqrt{S_1})}{\sqrt{S_1}} \left(\frac{1}{2} \sin 2\theta - \cos^2 \theta \cos \varphi \cos \Delta_{12} \right), \tag{8}
 \end{aligned}$$

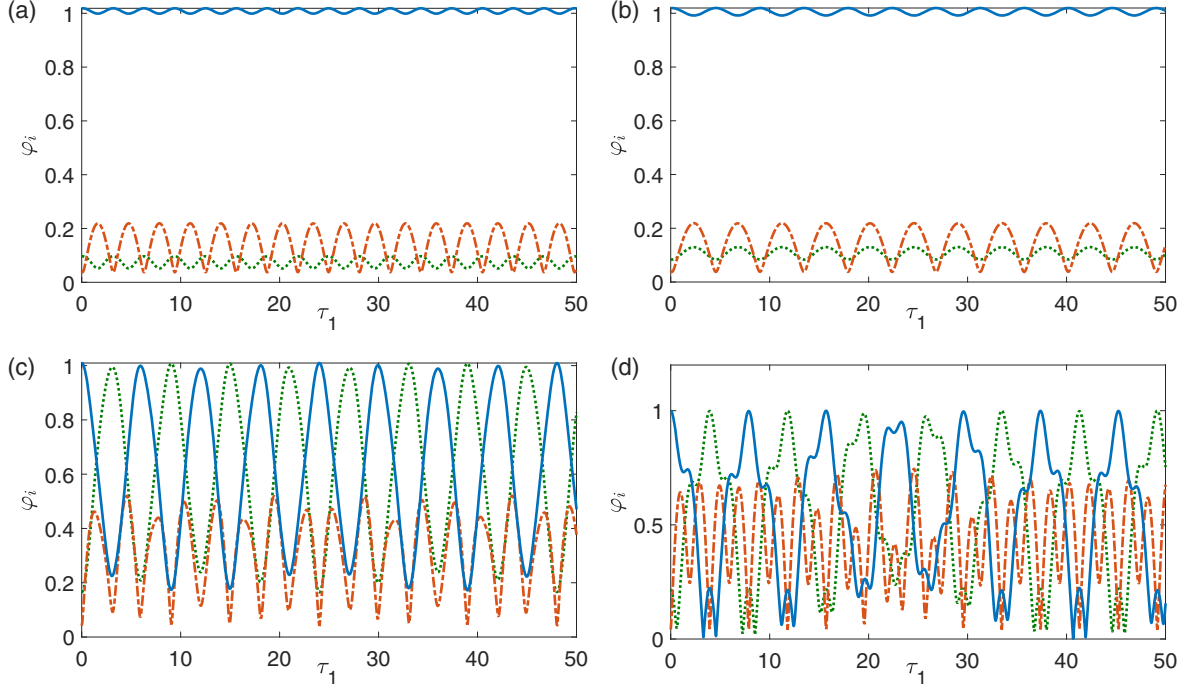


FIG. 5. Time evolutions of different regimes of system (4): $\theta = 1.53$, $\varepsilon = 0.1$, $\mu = 10$; (a) $\beta_0 = 0.5$, initial conditions correspond to C_1 ; (b) $\beta_0 = 0.5$, initial conditions correspond to C_2 ; (c) $\beta_0 = 2$, initial conditions correspond to C_3 ; (d) $\beta_0 = 2$, initial conditions correspond to C_4 . Blue solid line, red dashed line, and green dotted line denote φ_1 , φ_2 , φ_3 , respectively.

where $\Delta_{12} = \delta_1 - \delta_2$, $\Delta_{23} = \delta_2 - \delta_3$, $S_1 = \sin^2(\theta) + \cos^2(\theta)\cos^2(\varphi) - \sin(2\theta)\cos(\varphi)\cos(\Delta_{12})$, $S_2 = \sin^2(\theta) + \cos^2(\theta)\sin^2(\varphi) - \sin(2\theta)\sin(\varphi)\cos(\Delta_{23})$, $X = \frac{\omega}{2}Q^2$, and the Hamiltonian of the system is

$$H_{4D} = \mu \left[\frac{1}{4}Q^2\omega^2 - J_0(Q \sin \theta) - J_0(Q \cos \theta \cos \varphi) - J_0(Q \cos \theta \sin \varphi) \right] - \beta_0 J_0(Q\sqrt{S_1}) - \beta_0 J_0(Q\sqrt{S_2}). \quad (9)$$

The in-phase NNM and (1,0,-1) of system (2) in the new coordinates will correspond to the following solutions $(\theta, \phi, \Delta_{12}, \Delta_{23})$: $[\text{Arc cos}(\sqrt{\frac{2}{3}}), \frac{\pi}{4}, 0, 0]$ and $(0, \frac{\pi}{4}, 0, \pi)$, correspondingly.

It was shown for two pendula with the linear coupling [27] as well as the strongly nonlinear [37] coupling that the limiting phase trajectory (LPT) performs the key role in understanding the transitions between the energy exchange and its localization. LPT is a phase trajectory which corresponds to initial conditions when all the initial excitation is applied to one pendulum only; LPT demonstrates the maximum possible periodic energy exchange between the pendula for a given parameter set.

In the case of two pendula, the analysis of the reduced-order system can be performed on the phase plane. The phase plane can be presented as a periodic set of the rectangular cells centered by stationary points corresponding to NNMs. If the coupling parameter is high enough, the NNMs are stable, and the LPT represents the border of each cell and describes the full periodic recurrent energy exchange between the pendula, i.e., beatings. If the value of coupling parameter decreases, one of the NNMs loses its stability and two new asymmetric NNMs appear. However, the full energy exchange between the pendula is still possible. With the further decrease of the coupling parameter, the LPT collides with the separatrix

encircling the two new NNMs, and then the LPT undergoes a transformation and the dynamic phase transition occurs. The LPT amplitude decreases significantly and the full periodic energy exchange between the two oscillators is not possible. The LPT in the reduced phase space shows periodic amplitude modulations of oscillations of the initial system.

System (8) is four dimensional and its dimensionality can be reduced using Hamiltonian (9), but the system remains nonintegrable even in the slow timescale. However, the Poincaré section's analysis of the reduced system can be performed. The section plane was defined as $\theta = 1.53$ and Δ_{23} was defined from (9) as $H = h(\beta_0)$.

Because system (8) is not integrable, it may exhibit chaotic regimes. However, as it will become clear from the results shown below, there exist certain domains in the parametric space where the regular response regimes coexist with the nonregular ones. The intensive energy exchange regime (Fig. 6) shows the phase trajectory corresponding to the initial conditions for system (8):

$$\theta(0) = \varphi(0) = \Delta_{12}(0) = \Delta_{23}(0) = 0. \quad (10)$$

We call this regime the extended limiting phase trajectory by an analogy with the phase trajectory reflecting the evolution of the phase space in the system with two degrees of freedom (2DOF). It corresponds to the initial excitation of one

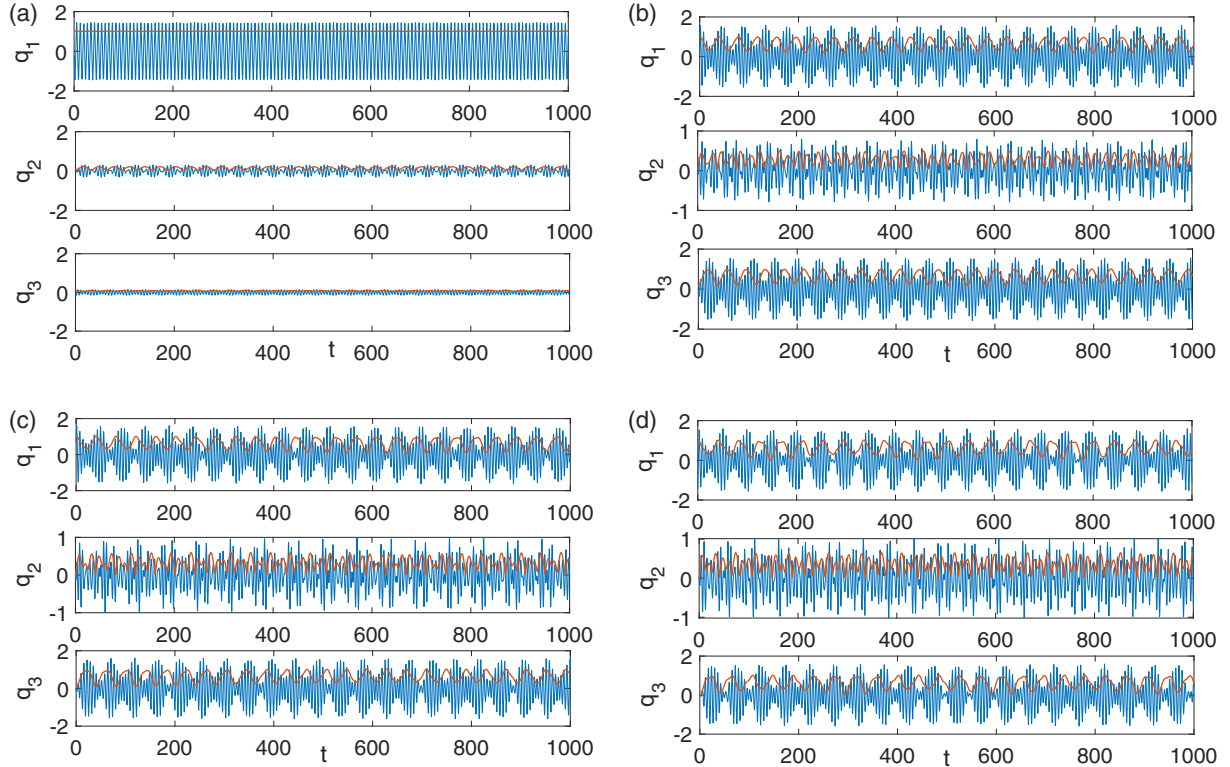


FIG. 6. Time history for the realization of the different regimes in system (1) (blue) and corresponding asymptotic system (4) (red): $\theta = 1.53$, $\varepsilon = 0.1$, $\mu = 10$; (a) $\beta = 0.05$, $\beta_0 = 0.5$, initial conditions correspond to C_1 ; (b) $\beta = 0.3$, $\beta_0 = 3$, initial conditions correspond to C_3 ; (c) $\beta = 0.3$, $\beta_0 = 3$, initial conditions correspond to one of the closed orbits of the Poincaré section [Fig. 4(f)]; (d) $\beta = 0.3$, $\beta_0 = 3$, initial conditions correspond to special orbit (10) ELPT.

of the side elements of the short chain. Using the conditions (10), we define the value of the integral $h(\beta_0)$ to show the ELPT on the Poincaré sections. Thus, we define the area of the phase space which can demonstrate the most intensive beating regime and the regimes which are close to it.

We have constructed Poincaré maps for different values of the coupling parameter β (see Fig. 4). For low values of coupling, the dynamics is regular; there are two stationary points on the map marked as C_1 and C_2 .

In the two-pendulum system, the Poincaré maps were constructed for an initial system in the fast timescale. Then stationary points of the Poincaré maps correspond to NNMs. However, in the case of the three pendula, the Poincaré sections are constructed for the reduced ordinary differential equations (ODE) set (8), where the evolution is considered in the slow timescale. Therefore, the stationary points correspond to periodic regimes in this timescale. They should correspond to the regimes of periodic energy exchange between the pendula of original system (2).

Both periodic dynamic states C_1 and C_2 are characterized by the strong energy localization of the energy on one (initially excited) side element. The two stationary points are encircled on the Poincaré map by the quasiperiodic orbits. As we will see, the red dots show the periodic orbit of the maximal amplitude in the Poincaré section; it corresponds to ELPT with quasiperiodic evolution in the slow timescale defined by initial conditions (10).

In the considered case, the regimes of the periodic energy exchange between the pendula (as well all quasiperiodic

trajectories between the extended LPT and the just mentioned stationary points) do not exactly satisfy the initial conditions corresponding to excitation of one oscillator only. However, the initial conditions for such regimes in the slow-flow system are very close to those for the ELPT. Therefore, we will keep the LPT denotation for the periodic trajectory corresponding to stationary point in the slow timescale. The time evolution for both periodic regimes in the slow timescale for weak coupling is presented in Figs. 5(a) and 5(b).

If the coupling increases, the chaotic regimes occupy most of the phase space [see Figs. 4(c) and 4(d)]; then a new periodic regime (denoted by C_3 at the section plane) of regular energy transport from one side element to another appears in the chaotic region [see Fig. 4(c)]. We remind the reader that this regime is called LPT, which is a phase trajectory that shows the possibility of the intensive regular energy exchange between the two edges of the short chain; the time evolution is seen in Fig 5(c). This stationary point remains in the Poincaré section with the further increase of the coupling parameter [Figs. 5(e) and 5(f)]. There are two stationary solutions on the map; other trajectories encircle them and correspond to the quasiperiodic motion of asymptotic slow-flow system (4). It is necessary to note that the stationary points corresponding to localization C_1 and C_2 , and to intensive energy exchange C_3 coexist on the Poincaré map in a narrow range of the coupling parameter.

The special orbit ELPT (10), being quasiperiodic for low values of coupling parameter, becomes chaotic when the coupling parameter increases [Fig. 4(d)]. When the coupling

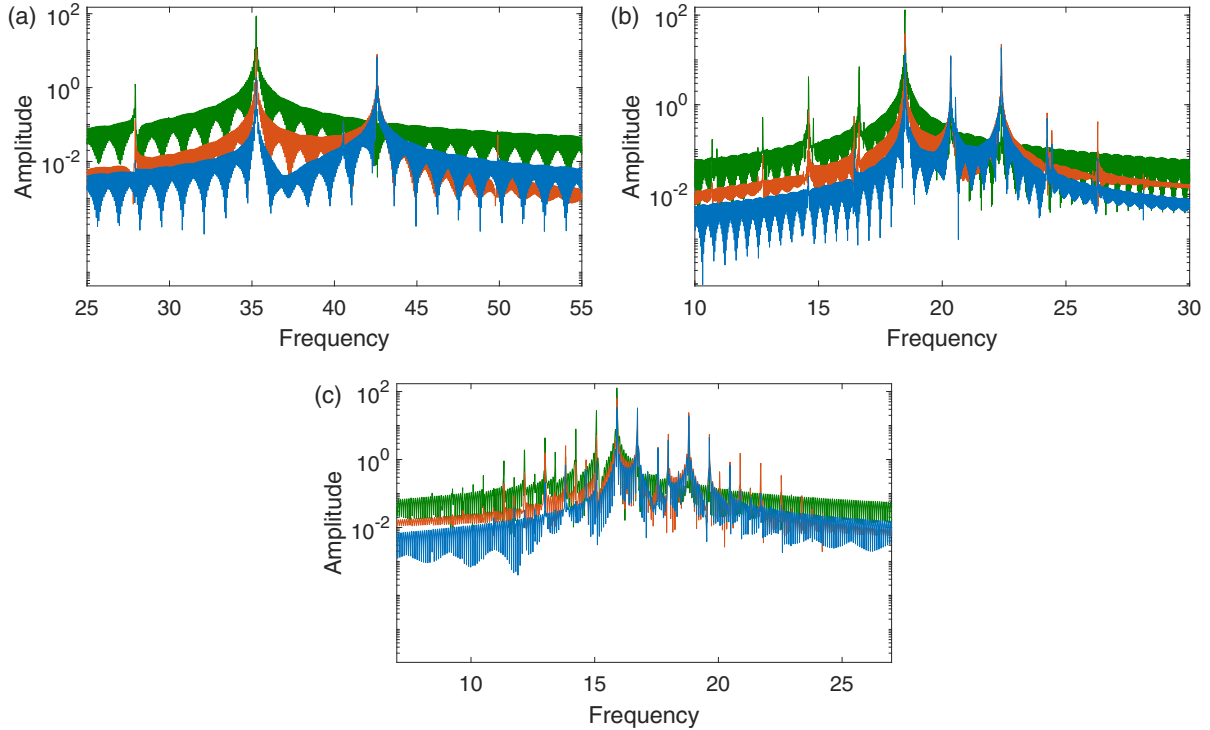


FIG. 7. Fast Fourier transform of the time histories for system (4), with the set of the initial conditions, corresponding to stationary point C_1 of the Poincaré section [see Fig. 4(a)]; (a) $\beta = 0.05$; (b) $\beta = 0.1$; (c) $\beta = 0.12$. Green color, upper curve denotes φ_1 ; red color, middle curve denotes φ_2 ; and blue color, lower curve denotes φ_3 .

parameter is further increased, ELPT again appears to be quasiperiodic [see Figs. 4(e) and 4(f)], but encircles another dynamical regime—the regime of intensive energy beating between the two edge elements. In the Poincaré maps study of the 2DOF system, the transition through the chaotic region also corresponds to the dynamical transition from energy localization to energy exchange regime.

In both cases of two and three coupled pendula, the LPT shows the maximum possible regular energy exchange between the edge elements of the short chain. For high values of the coupling parameter, the LPT demonstrates the intensive regular beatings, while for low values of the coupling parameter, it corresponds to the dynamical regimes with small-amplitude modulations of the state localized on one side element.

To verify the regimes obtained in the study of the reduced-order system, we compare the time evolution of the initial system of three pendula with the evolution of the envelope functions, both with initial conditions corresponding to the stationary points of the Poincaré sections (see Fig. 4). It is obvious that the dimensionality of the asymptotic system is reduced in comparison with the initial one. This means that asymptotic system (8) as well as (4) can demonstrate regular motions at the initial conditions which correspond to the chaotic motion of the full system. To check the correspondence between the regimes obtained in the Poincaré maps study of the reduced-order system, we have thoroughly studied the evolution of the full system for different values of the initial conditions and for different values of the coupling parameter. In order to demonstrate the behavior of full system

(2) in Fig. 5, we present displacement evolution with time under parameter sets and initial conditions corresponding to stationary points of the Poincaré sections [Figs. 4(a) and 4(f)]. We also show the evolution of special orbit ELPT (10) and the evolution of some phase trajectory corresponding to one closed orbit of the Poincaré section [Fig. 4(f)]. We should mention that the different type of LPTs can be reported now, namely, the LPT with quasiperiodic slow timescale evolution.

It is seen in Fig. 5 that the stationary point of the Poincaré section can be associated with the periodic regime of the slow flow as well as with the quasiperiodic one. Evidently enough, the periodic motion of the reduced system should correspond to the quasiperiodic or the motion with two characteristic frequencies, namely, frequency of the fast oscillations and frequency of the slow envelope-function evolution (see Fig. 6). However, the Fourier spectra obtained using the fast Fourier transformation demonstrate that the additional frequencies appear in the spectrum of the time evolution with the growth of the coupling parameter β . They help us to report on the quasiperiodic motion in the slow system with initial conditions corresponding to the stationary point of the Poincaré section (for example, C_1 in Fig. 7 and C_3 in Fig. 8). This happens due to the presence of the multiple frequencies which do not show themselves in the Poincaré sections. The reason for their appearance is the essential nonlinearity of the system that makes the processes of nonstationary energy localization as well as energy transport in the system a much more complex process in comparison to the one in the system of the quasilinear coupled oscillators [39]. We demonstrate then the basic frequency of the fast oscillations and the main

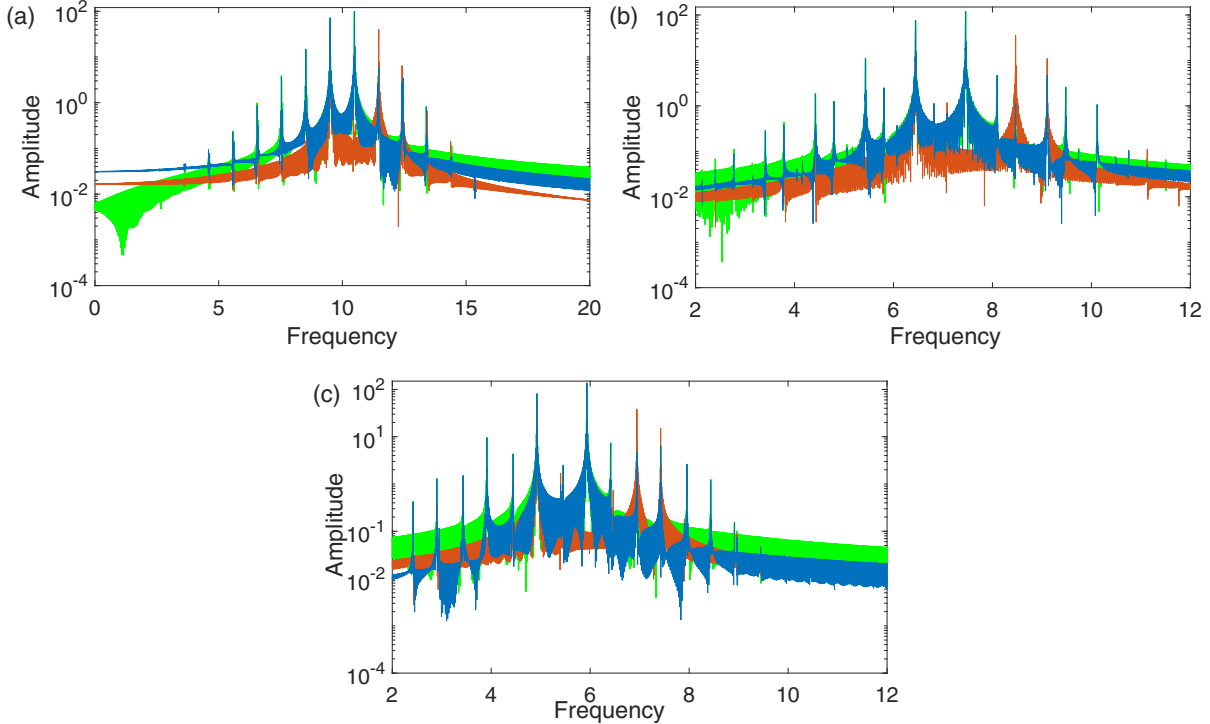


FIG. 8. Fast Fourier transform of the time histories for system (4), with the set of the initial conditions, corresponding to stationary point C_3 of the Poincaré section [see Fig. 4(c)]; (a) $\beta = 0.2$; (b) $\beta = 0.3$; (c) $\beta = 0.4$. Green color denotes φ_1 , red color denotes φ_2 , and blue color denotes φ_3 .

frequency of the periodic motion in the slow timescale. Please note that for the initial conditions corresponding to C_3 , the basic frequency of the slow motion can be observed in the spectra for each of the oscillators (the high peak visible for all the oscillators), while the frequency of the periodic energy exchange (high peak on the right-hand side from the main frequency) can be observed only for two side elements. In agreement with the time-evolution profiles, we see that the relative frequency of the time modulation of the middle element is two times higher than the frequencies of the modulations of the side elements. More detailed analysis of the spectra is beyond the scope of this contribution.

IV. DISCUSSION AND CONCLUSIONS

We report the study of the nonstationary dynamics in the system of three pendula coupled by the cosine potential. Based on the numeric evidence, we conclude (under the conditions of the initial loading concentrated mainly on one of the side-pendula) that with the growth of the coupling parameter, the transition from the energy localization on the initially excited pendulum to recurrent energy exchange between the two side pendula occurs. Using the asymptotic procedure which already was applied for the system of two linearly coupled pendula [27], we reduce the system to the form when the Poincaré sections analysis is possible.

We verify the applicability of the asymptotic procedure checking the analytical dependence of the two resonating NNMs on the amplitude of the initial excitation. It is seen that if the coupling parameter is small enough, the frequencies of two NNMs are close to each other.

We report that similarly to the system of two nonlinearly coupled pendula [37], the inversion of the spectrum is observed with growth of the amplitude of initial excitation. This phenomenon is not observed for the system with linear coupling [27]. We also provide the stability analysis of the NNMs. Using the reduced-order model, we show that the transition from dynamic regimes of energy localization to recurrent energy transport is not connected with the change of stability of one of the resonating NNMs, but with instability of the LPT corresponding to the maximum possible periodic energy exchange in the conditions of predominant energy localization on the initially excited pendulum.

The analysis of Poincaré sections can be made based on the LPT concept. The evolution of the Poincaré section shows that similarly to the system of two linearly coupled pendula, the transition of LPT through the chaotic region of the phase space leads to the significant change of the response in the case of the strongly asymmetric initial loading, i.e., from energy localization to recurrent energy exchange.

It should be also noted that while for two weakly coupled pendula the LPT corresponds to full interpendulum energy exchange, in the case of three pendula, one has to differ the periodic LPTs with almost full energy exchange between the edge pendula and quasiperiodic orbits. We call the outer one on the phase space the ELPT, which corresponds to the full energy exchange between these pendula.

The physical meaning of the regime with excitation mostly localized on the side element is similar to that of the discrete breather in the long chain of nonlinear oscillators [35]. In the short chains of rotors [32], such solutions are reported

to appear with intensive excitation of the middle element; however, in our case, only the solution localized on the edge element is observed.

We also emphasize that in the current study, we report on the high-dimensional analogue of the classical beatings phenomenon between the two oscillators. Due to lower dimensionality in the system of two pendula, it demonstrates regular periodic intensive energy exchange between the two oscillators. In the earlier works, the intensive beatings were reported in the systems with more than two degrees of freedom with the periodic boundary conditions, but they characterize the energy exchange between the coherent domains or clusters of the system [30,31]. The present work extends the phenomenon of

the intensive periodic energy exchange between the two ends of the short oscillatory chains with more than two degrees of freedom.

ACKNOWLEDGMENTS

M.K. is thankful to the Russian Foundation for Basic Research for financial support (Grant No. 16-33-60186). In the paper are discussed the results of the study of the system of two pendula with nonlinear coupling which are obtained in the framework of the Program of Fundamental Researchers of the Russian State Academies of Sciences 2013–2020 (Project No. 0082-2014-0013).

-
- [1] N. Bogoliubov and Y. A. Mitropolsky, *Asymptotic Methods in the Theory of Non-Linear Oscillations* (Gordon & Breach, New York, 1961).
- [2] Io. G. Malkin, *Theory of Stability of Motion* (University of Michigan Library, Michigan, 1958).
- [3] R. Z. Sagdeev, D. A. Usikov, and G. M. Zaslavsky, *Nonlinear Physics* (Harwood, New York, 1988).
- [4] J. K. Hale, *Oscillations in Nonlinear Systems* (Mc. Graw-Hill, New York, 1963).
- [5] M. Toda, Studies of a nonlinear lattice, *Phys. Rep.* **18**, 1 (1975).
- [6] O. M. Braun and Yu. Kivshar, *The Frenkel-Kontorova Model. Concepts, Methods, and Applications* (Springer Science & Business Media, New York, 2004).
- [7] Al. F. Vakakis, L. I. Manevitch, Yu. V. Mikhlin, V. N. Pilipchuk, and Al. A. Zevin, *Normal Modes and Localization in Nonlinear Systems* (Kluwer Academic, Dordrecht, 2008).
- [8] I. N. Barabanov and V. N. Tkhai, Oscillation family in weakly coupled identical systems, *Autom. Remote Control* **77**, 561 (2016).
- [9] V. N. Tkhai, Oscillations, stability and stabilization in the model containing coupled subsystems with cycles, *Autom. Remote Control* **76**, 1169 (2015).
- [10] I. N. Barabanov, A. T. Tureshbaev, and V. N. Tkhai, Basic oscillation mode in the coupled-subsystems model, *Autom. Remote Control* **75**, 2112 (2014).
- [11] A. P. Kuznetsov, L. V. Turukina, N. Yu. Chernyshov, and Yu. V. Sedova, Oscillations and synchronization in a system of three reactively coupled oscillators, *Int. J. Bifurcation Chaos Appl. Sci. Eng.* **26**, 1650010 (2016).
- [12] A. P. Kuznetsov, I. R. Sataev, and L. V. Tyuryukina, Synchronization of quasi-periodic oscillations in coupled phase oscillators, *Tech. Phys. Lett.* **36**, 478 (2010).
- [13] L. V. Turukina and A. Pikovsky, Hyperbolic chaos in a system of resonantly coupled weakly nonlinear oscillators, *Phys. Lett. A* **375**, 1407 (2011).
- [14] A. P. Kuznetsov, S. P. Kuznetsov, and Yu. V. Sedova, Pendulum system with an infinite number of equilibrium states and quasiperiodic dynamics, *Rus. J. Nonlin. Dyn.* **12**, 223 (2016).
- [15] A. Pikovsky, M. Rosenblum, and J. Kurths, *Synchronization. A Universal Concept in Nonlinear Sciences* (Cambridge University Press, Cambridge, 2001).
- [16] Al. L. Fradkov and B. Andrievsky, Synchronization and phase relations in the motion of two-pendulum system, *Intl. J. Non-Linear Mech.* **42**, 895 (2007).
- [17] D. Bitar, N. Kacem, and N. Bouhaddi, Investigation of modal interactions and their effects on the nonlinear dynamics of a periodic coupled pendulums chain, *Int. J. Mech. Sci.* **127**, 130 (2017).
- [18] A. Najdecka, T. Kapitaniak, and M. Wiercigroch, Synchronous rotational motion of parametric pendulums, *Int. J. Non-Lin. Mech.* **70**, 84 (2015).
- [19] A. P. Markeev, On the stability of nonlinear vibrations of coupled pendulums, *Mech. Solids* **48**, 370 (2013).
- [20] A. P. Markeev, A motion of connected pendulums, *Rus. J. Nonlin. Dyn.* **9**, 27 (2013).
- [21] L. I. Manevitch, New approach to beating phenomenon in coupled nonlinear oscillatory chains, *Arch. Appl. Mech.* **77**, 301 (2007).
- [22] A. Kovaleva, L. I. Manevitch, and E. L. Manevitch, Intense energy transfer and superharmonic resonance in a system of two coupled oscillators, *Phys. Rev. E* **81**, 056215 (2010).
- [23] A. Kovaleva and L. I. Manevitch, Limiting phase trajectories and emergence of autoresonance in nonlinear oscillators, *Phys. Rev. E* **88**, 024901 (2013).
- [24] L. I. Manevitch and V. V. Smirnov, Resonant energy exchange in nonlinear oscillatory chains and limiting phase trajectories: from small to large systems, in *Advanced Nonlinear Strategies for Vibration Mitigation and System Identification*, edited by A. F. Vakakis (Springer, Berlin, 2010), pp. 207–258.
- [25] L. I. Manevitch, A. Kovaleva, E. L. Manevitch, and D. S. Shepelev, Limiting phase trajectories and non-stationary resonance oscillations of the Duffing oscillator. Part 1. A non-dissipative oscillator, *Commun. Nonlinear Sci. Numer. Simul.* **16**, 1089 (2011).
- [26] L. I. Manevitch, A. Kovaleva, E. L. Manevitch, and D. S. Shepelev, Limiting phase trajectories and non-stationary resonance oscillations of the Duffing oscillator. Part 2. A dissipative oscillator, *Commun. Nonlinear Sci. Numer. Simul.* **16**, 1098 (2011).
- [27] L. I. Manevitch and F. Romeo, Non-stationary resonance dynamics of weakly coupled pendula, *Europhys. Lett.* **112**, 30005 (2015).
- [28] Sh. Takeno and S. Homma, A sine-lattice (sine-form discrete sine-Gordon) equation—one- and two-kink solutions and physical models, *J. Phys. Soc. Jpn.* **55**, 65 (1986).
- [29] S. Yomosa, Soliton excitations in deoxyribonucleic acid (DNA) double helices, *Phys. Rev. A* **27**, 2120 (1983).

- [30] L. I. Manevitch and V. V. Smirnov, Limiting phase trajectories and the origin of energy localization in nonlinear oscillatory chains, *Phys. Rev. E* **82**, 036602 (2010).
- [31] V. V. Smirnov and L. I. Manevitch, Limiting phase trajectories and dynamic transitions in nonlinear periodic systems, *Acoust. Phys.* **57**, 271 (2011).
- [32] N. Cuneo, J. P. Eckmann, and C. Poquet, Non-equilibrium steady state and subgeometric ergodicity for a chain of three coupled rotors, *Nonlinearity* **28**, 2397 (2015).
- [33] N. Cuneo and J. P. Eckmann, Non-equilibrium steady states for chains of four rotors, *Commun. Math. Phys.* **345**, 185 (2016).
- [34] N. Cuneo, J. P. Eckmann, and C. E. Wayne, Energy dissipation in hamiltonian chains of rotators, *Nonlinearity* **30**, R81 (2017).
- [35] S. Flach and A. V. Gorbach, Discrete breathers—advances in theory and applications, *Phys. Rep.* **467**, 1 (2008).
- [36] V. V. Smirnov and L. I. Manevitch, Semi-inverse method in nonlinear mechanics: application to couple shell- and beam-type oscillations of single-walled carbon nanotubes, *Nonlinear Dynamics* **93**, 205 (2018).
- [37] M. A. Kovaleva, V. V. Smirnov, and L. I. Manevitch, Stationary and nonstationary dynamics of the system of two harmonically coupled pendulums, *Rus. J. Nonlin. Dyn.* **13**, 105 (2017).
- [38] V. Kislovsky, M. Kovaleva, K. R. Jayaprakash, and Y. Starosvetsky, Consecutive transitions from localized to delocalized transport states in the anharmonic chain of three coupled oscillators, *Chaos* **26**, 073102 (2016).
- [39] L. I. Manevitch, A. S. Kovaleva, V. V. Smirnov, and Yu. Starosvetsky, *Nonstationary Resonant Dynamics of Oscillatory Chains and Nanostructures* (Springer Nature, Singapore, 2017), p. 436.